V European Conference on Computational Fluid Dynamics
ECCOMAS CFD 2010
J. C. F. Pereira and A. Sequeira (Eds)
Lisbon, Portugal,14-17 June 2010

CHARACTERISTIC BASED NONREFLECTING BOUNDARY CONDITIONS IN A SIMPLE-TYPE PRESSURE CORRECTION ALGORITHM FOR LOW MACH NUMBER FLOWS

Y. Moguen[†], T. Kousksou[††], E. Dick[*] and P. Bruel[†††]

[†]Université de Pau et des Pays de l'Adour - Laboratoire de Sciences Appliquées au Génie Civil et Côtier,
ISA-BTP, avenue du Parc Montaury - 64 600 Anglet, France
e-mail: yann.moguen@free.fr
[††]Université de Pau et des Pays de l'Adour - Laboratoire de Thermique, Énergétique et Procédés
ENSGTI, rue Jules Ferry - 64 075 Pau, France
e-mail: tarik.kousksou@univ-pau.fr
[*]Universiteit Gent - Vakgroep Mechanica van stroming, warmte en verbranding
Sint-Pietersnieuwstraat, 41 - 9 000 Gent, Belgium
e-mail: erik.dick@ugent.be
[†††]CNRS and Université de Pau et des Pays de l'Adour - Laboratoire de Mathématiques et de leurs Applications, UMR 5142 CNRS-UPPA
avenue de l'Université, BP 1155 - 64 013 Pau, France
e-mail: pascal.bruel@univ-pau.fr

Key words: Nonreflecting boundary conditions, Pressure correction, Low Mach number flow

Abstract. *The combination of nonreflective boundary conditions with SIMPLE-type algorithms is not straightforward, due to the time staggered treatment of the physical variables in these algorithms. First, a model algorithm is described, such as to bring together classical features of SIMPLE-type approaches for compressible flows. As we focus on low Mach number computations, the $AUSM^+$-up scheme is utilized, but this does not restrict the suggested methodology, which consists in applying characteristic based boundary conditions according to the physical role played by the variables that are concerned.*

1 INTRODUCTION

When dealing with flow models which require the radiation of waves into the far field, nonreflecting boundary conditions must be introduced. Even in steady computations, convergence problems may occur otherwise. In unsteady computations, nonphysical reflections can render the simulation useless, in particular when the interaction of sound waves with fluid flows is of interest. Particular care has to be applied to the boundary conditions treatment at low Mach number, since multiple time scales are then involved with different orders of magnitude. In this case, accurate boundary conditions are needed for 'long' times measured on the 'fast' scale.

The vast literature on nonreflecting boundary conditions is essentially divided into two streams treating either absorbing or characteristic boundary treatment. According to the former approach, a nonphysical buffer zone is added to the physical domain. This was found particularly necessary when nonlinear disturbances, such as vortices, cross the boundary. When only acoustic waves must exit the computational domain with minimal reflections, characteristic based boundary treatment has been shown to be highly effective (see *e.g.* [10, 12, 9, 1]).

In the present study we examine the characteristic boundary treatment in SIMPLE-type pressure correction algorithms. These algorithms are characterized by a procedure in which the pressure field is decomposed into a guessed value and a pressure correction, which is related to a momentum correction by an approximate form of the momentum equation. As far as pressure correction algorithms are concerned, the energy-based approach has been shown to be suitable when low Mach number flows must be accurately computed. Because we shall focus on low Mach number flows, this approach will be adopted. We note, however, that the energy-based SIMPLE-type pressure correction methods have been used successfully to solve flow problems for a wide range of Mach number[13,7,8,3]. The methodology that we shall describe in the present study is aimed at this class of methods, and more generally at the SIMPLE-type approach for compressible flows.

Specific difficulties arise when characteristic based nonreflecting boundary conditions are applied in the algorithms which belong to the class that we consider. In the estimation step, pressure is frozen, which means that acoustic information is involved only in the correction step. Thus, physical variables are staggered in time, depending on the convective or acoustic roles they play. This is why a nonreflecting treatment is not straightforward, in contrast to the case of explicit time marching schemes commonly combined with this treatment.

Let us note that the topic that we consider remains a very seldom studied subject. However, in Ref. [14], the nonreflecting conditions technique given in [9] is applied in a SIMPLE-type pressure correction algorithm in which the pressure correction is derived from a Helmholtz equation. A LES computation is performed with a Mach number of 0.04 at the inlet and a time step that corresponds to an acoustic CFL as large as 40. It

will be of interest to discuss the stability features of the method that we shall present with regard to this result.

The organization of this paper is as follows. First, an algorithm designed to represent a large class of pressure correction algorithms is described. Without intending to investigate its particular features or capabilities, particularly for the low Mach aspects, we utilize it as a generic – or model – algorithm, that brings together classical features of SIMPLE-type approaches for compressible flows, such as the distinction between convective and acoustic variables, and the use of a pressure and momentum correction relation derived from the momentum equation.

Second, after recalling some well-known aspects of characteristic based boundary conditions, their integration into our model pressure correction scheme is presented. The method that we suggest here, consists in applying the characteristic based boundary conditions in a staggered way too, according to the physical role of the variables that are concerned. The suggested methodology is tested on two cases: steady flow in a nozzle with variable section and acoustic wave packet propagation. The time step limitation of the described method is then discussed.

2 GOVERNING EQUATIONS

We consider the simple case of a one-dimensional flow of a perfect and ideal gas in a nozzle with a variable section. From now on, x denotes the coordinate in the flow direction. The flow model is given by the Euler equations,

$$\partial_t(\varrho S) + \partial_x(\varrho v S) = 0 \tag{1a}$$

$$\partial_t(\varrho v S) + \partial_x((\varrho v^2 + p)S) = p\mathrm{d}_x S \tag{1b}$$

$$\partial_t(\varrho E S) + \partial_x(\varrho v H S) = 0 \tag{1c}$$

$$E = e + \frac{1}{2}v^2 \tag{1d}$$

$$\varrho H = \varrho E + p \tag{1e}$$

$$\varrho e = \frac{p}{\gamma - 1} \tag{1f}$$

where t, ϱ, p, v, e, E and H represent time, density, pressure, velocity, internal energy, total energy and total enthalpy per unit mass, respectively. Furthermore, γ denotes the specific heats ratio and S the cross-section area of the nozzle.

For numerical reasons, it is usual to put the variables in nondimensional form. Let us introduce a pressure p_r, density ϱ_r and length l_r, as three fundamental reference quantities. From these, we deduce a reference velocity $v_r = \sqrt{p_r/\varrho_r}$, time $t_r = l_r/v_r$, energies and total enthalpy $e_r = E_r = H_r = p_r/\varrho_r$. We thus define nondimensionalized quantities, which satisfy the set of equations (1) as well. The same symbols are used for the dimensionless variables as for the dimensional ones.

The x axis along the nozzle is divided into a number N of cells of length Δx, in the

center of which the variables are stored. The boundaries of the computational domain coincide with the first and the last centers, that correspond to $i = 1$ and $i = N$, respectively.

3 A MODEL PRESSURE CORRECTION ALGORITHM

In this section, an energy-based SIMPLE-type pressure correction algorithm is described. As we are interested in low Mach number flows computations, the AUSM$^+$-up interpolation scheme is utilized[4]. It is combined with the pressure correction procedure in an original manner, designed with the goal to introduce the mass flux-pressure link through the explicitly given level of numerical dissipation contained in the AUSM$^+$-up scheme exclusively[5]. But the choice of the interpolation scheme does not affect the generic character of the proposed algorithm concerning the problem of its combination with a nonreflecting treatment.

3.1 Methodology

From now on, the superscripts $\star$ and $\prime$ denote respectively estimated and correction quantities. First, we recall some technical aspects of the AUSM$^+$-up scheme. We refer to [4] for further details and explanations. The critical speed of sound is evaluated as

$$\overline{c}_i^\star = \sqrt{\frac{2(\gamma-1)H_i^\star}{\gamma+1}} \tag{2}$$

Then the interface speed of sound is

$$c_{i+1/2}^\star = \min\{\tilde{c}_i^\star, \tilde{c}_{i+1}^\star\} \tag{3}$$

where

$$\tilde{c}_i^\star = \frac{(\overline{c}_i^\star)^2}{\max\{\overline{c}_i^\star, v_i^k\}} \tag{4}$$

An estimated Mach number on cells i and $i+1$ is defined as

$$M_i^\star = \frac{v_i^k}{c_{i+1/2}^\star} \quad , \quad M_{i+1}^\star = \frac{v_{i+1}^k}{c_{i+1/2}^\star} \tag{5}$$

where, from now on, the superscript k denotes a known iteration level, such that $k = n$ at the first estimation-correction sequence. An estimated mean local Mach number is

$$\overline{M}_{i+1/2}^\star = \sqrt{\frac{(v_i^k)^2 + (v_{i+1}^k)^2}{2(c_{i+1/2}^\star)^2}} \tag{6}$$

A reference Mach number $M_{0,i+1/2}^\star$ is defined by

$$(M_{0,i+1/2}^\star)^2 = \min\{1, \max\{(\overline{M}_{i+1/2}^\star)^2, \mathrm{Ma}_{\mathrm{co}}^2\}\} \tag{7}$$

where $\mathrm{Ma_{co}}$ is a cut-off Mach number such that: $\mathrm{Ma_{co}} = \mathcal{O}(\mathrm{Ma}_\infty)$. A scaling function suggested in Ref. [4] is

$$f_c(M^\star_{0,i+1/2}) = M^\star_{0,i+1/2}(2 - M^\star_{0,i+1/2}) \tag{8}$$

This scaling function is a simplification of the one given in Ref. [2]. In this reference, the scaling function was used to define a preconditioned Mach number by introducing a preconditioned speed of sound. In the present approach, we do not use a preconditioned Mach number for the face velocity. We only use the scaling function to ensure the proper asymptotic behaviour of the pressure dissipation term in the face mass flux, as described below.

Now, we introduce the following functions utilized in the interpolations,

$$M^\pm_{(1)}(M) = \frac{1}{2}(M \pm |M|) \tag{9}$$

$$M^\pm_{(4)}(M) = \pm\frac{1}{4}(M \pm |M|)^2 \pm \frac{1}{8}(M^2-1)^2 \tag{10}$$

$$P^\pm_{(0)}(M) = M^\pm_{(1)}(M)/M \tag{11}$$

$$P^\pm_{(5)}(M) = \frac{1}{4}(M \pm 1)^2(2 \mp M) \pm \frac{3}{16}(5(f_c(M_0))^2 - 4)M(M^2-1)^2 \tag{12}$$

Then,

$$\mathcal{M}^\pm(M) = \begin{cases} M^\pm_{(1)}(M) & , \quad |M| \geq 1 \\ M^\pm_{(4)}(M) & , \quad |M| < 1 \end{cases} \tag{13}$$

and

$$\mathcal{P}^\pm(M) = \begin{cases} P^\pm_{(0)}(M) & , \quad |M| \geq 1 \\ P^\pm_{(5)}(M) & , \quad |M| < 1 \end{cases} \tag{14}$$

The estimated interface Mach number is defined as

$$M^\star_{i+1/2} = \mathcal{M}^+(M^\star_i) + \mathcal{M}^-(M^\star_{i+1}) - \frac{K_p}{f_c(M^\star_{0,i+1/2})} \max\{1 - (\overline{M}^\star_{i+1/2})^2\sigma, 0\} \, \frac{p^k_{i+1} - p^k_i}{\varrho^\star_i (c^\star_{i+1/2})^2} \tag{15}$$

where K_p and σ are two constants.

The estimated mass flux and velocity at the interface are given by the AUSM$^+$-up scheme,

$$(\varrho v)^\star_{i+1/2} = c^\star_{i+1/2} \; M^\star_{i+1/2} \; \varrho^\star_i \tag{16}$$

and

$$v^\star_{i+1/2} = c^\star_{i+1/2} \; M^\star_{i+1/2} \tag{17}$$

Accordingly, the mass flux correction is also expressed as

$$(\varrho v)'_{i+1/2} = c^\star_{i+1/2} \; M'_{i+1/2} \; \varrho^\star_i \tag{18}$$

where

$$M'_{i+1/2} = -\frac{K_p}{f_c(M^\star_{0,i+1/2})} \max\{1 - (\overline{M}^\star_{i+1/2})^2\sigma, 0\} \ \frac{p'_{i+1} - p'_i}{\varrho^\star_i (c^\star_{i+1/2})^2} \tag{19}$$

To compute the pressure correction p', a key role is assigned to the energy equation. For an Euler-implicit discretization, it reads as

$$(\varrho E)^{n+1}_i - (\varrho E)^n_i + \frac{\tau}{S_i}\left\{(\varrho v H)^{n+1}_{i+1/2} S_{i+1/2} - (\varrho v H)^{n+1}_{i-1/2} S_{i-1/2}\right\} = 0 \tag{20}$$

where τ is formally defined as $\Delta t/\Delta x$. The total energy is expanded as

$$(\varrho E)^{n+1}_i = (\varrho E)^\star_i + (\partial_p(\varrho e))^\star_i p'_i \tag{21}$$

In the case of a perfect gas,

$$(\partial_p(\varrho e))^\star_i = \frac{1}{\gamma - 1} \tag{22}$$

The flux term is expanded as

$$(\varrho v H)^{n+1}_{i+1/2} = (\varrho H)^\star_i v^\star_{i+1/2} + H^\star_i (\varrho v)'_{i+1/2} + (\varrho H)'_{i+1/2} v^\star_{i+1/2} \tag{23}$$

where the convected quantity $(\varrho H)^\star_{i+1/2}$ is upwinded as $(\varrho H)^\star_i$.

Now, each term of the previous expansion has to be related to pressure corrections.

The interface total enthalpy correction is

$$(\varrho H)'_{i+1/2} = (\varrho E)'_{i+1/2} + p'_{i+1/2} = \frac{\gamma}{\gamma - 1} p'_{i+1/2} \tag{24}$$

where the interface pressure correction is defined as

$$p'_{i+1/2} = \mathcal{P}^+(M^\star_i) p'_i + \mathcal{P}^-(M^\star_{i+1}) p'_{i+1} \tag{25}$$

while the following interpolation formula stands for the interface pressure,

$$\begin{aligned} p_{i+1/2} = {} & \mathcal{P}^+(M_i) p_i + \mathcal{P}^-(M_{i+1}) p_{i+1} \\ & - K_v \mathcal{P}^+(M_i)\mathcal{P}^-(M_{i+1})(\varrho_i + \varrho_{i+1})(f_c(M_{0,i+1/2}) c_{i+1/2})(v_{i+1} - v_i) \end{aligned} \tag{26}$$

where K_v is a positive constant.

Thus, the energy equation (20) becomes

$$
\begin{aligned}
&(\varrho E)_i^\star + \frac{1}{\gamma-1}p'_i - (\varrho E)_i^n \\
&\quad + \frac{\tau}{S_i}[(\varrho H)_i^\star c_{i+1/2}^\star M_{i+1/2}^\star S_{i+1/2} - (\varrho H)_{i-1}^\star c_{i-1/2}^\star M_{i-1/2}^\star S_{i-1/2}] \\
&\quad + \frac{\tau}{S_i}\{[\frac{\gamma}{\gamma-1}(\mathcal{P}^+(M_i^\star)p'_i + \mathcal{P}^-(M_{i+1}^\star)p'_{i+1})c_{i+1/2}^\star M_{i+1/2}^\star \\
&\quad - H_i^\star \frac{K_p}{f_c(M_{0,i+1/2}^\star)}\max\{1-(\overline{M}_{i+1/2}^\star)^2\sigma, 0\}\frac{p'_{i+1}-p'_i}{c_{i+1/2}^\star}]S_{i+1/2} \\
&\quad - [\frac{\gamma}{\gamma-1}(\mathcal{P}^+(M_{i-1}^\star)p'_{i-1} + \mathcal{P}^-(M_i^\star)p'_i)c_{i-1/2}^\star M_{i-1/2}^\star \\
&\quad - H_{i-1}^\star \frac{K_p}{f_c(M_{0,i-1/2}^\star)}\max\{1-(\overline{M}_{i-1/2}^\star)^2\sigma, 0\}\frac{p'_i-p'_{i-1}}{c_{i-1/2}^\star}]S_{i-1/2}\} = 0
\end{aligned} \tag{27}
$$

Finally, as in every algorithm which belongs to the SIMPLE family, a relationship between momentum correction and pressure correction has to be constructed. First, the momentum estimation is given by the first-order upwinded equation,

$$
(\varrho v)_i^\star = (\varrho v)_i^n - \frac{\tau}{S_i}\left((\varrho v)_i^\star v_{i+1/2}^k S_{i+1/2} - (\varrho v)_{i-1}^\star v_{i-1/2}^k S_{i-1/2}\right) - \tau(p_{i+1/2}^k - p_{i-1/2}^k) \tag{28}
$$

Substracting Eq. (28) from the upwinded Euler-implicit discretization of the momentum equation,

$$
\begin{aligned}
(\varrho v)_i^{n+1} = (\varrho v)_i^n &- \frac{\tau}{S_i}[(\varrho v)_i^{n+1} v_{i+1/2}^{n+1} S_{i+1/2} - (\varrho v)_{i-1}^{n+1} v_{i-1/2}^{n+1} S_{i-1/2}] \\
&- \tau(p_{i+1/2}^{n+1} - p_{i-1/2}^{n+1})
\end{aligned} \tag{29}
$$

one has

$$
\begin{aligned}
(\varrho v)'_i = -\frac{\tau}{S_i}\{&[(\varrho v)_i^{n+1} v_{i+1/2}^{n+1} - (\varrho v)_i^\star v_{i+1/2}^k]S_{i+1/2} \\
&- [(\varrho v)_{i-1}^{n+1} v_{i-1/2}^k - (\varrho v)_{i-1}^\star v_{i-1/2}^k]S_{i-1/2}\} - \tau(p'_{i+1/2} - p'_{i-1/2})
\end{aligned} \tag{30}
$$

Neglecting products of corrections,

$$
(\varrho v)_i^{n+1} v_{i+1/2}^{n+1} = (\varrho v)_i^\star v_{i+1/2}^k + (\varrho v)_i^\star v'_{i+1/2} + (\varrho v)'_i v_{i+1/2}^k \tag{31}
$$

we obtain

$$
\begin{aligned}
(\varrho v)'_i = -\frac{\tau}{S_i}&[(\varrho v)'_i v_{i+1/2}^k S_{i+1/2} - (\varrho v)'_{i-1} v_{i-1/2}^k S_{i-1/2}] \\
&- \frac{\tau}{S_i}[(\varrho v)_i^\star v'_{i+1/2} S_{i+1/2} - (\varrho v)_{i-1}^\star v'_{i-1/2} S_{i-1/2}] - \tau(p'_{i+1/2} - p'_{i-1/2})
\end{aligned} \tag{32}
$$

As an extreme simplification of (32), we take here

$$
(\varrho v)'_i = -\tau(p'_{i+1/2} - p'_{i-1/2}) \tag{33}
$$

3.2 Algorithm

The estimation-correction loop takes the following form:

• Initializations: ϱ_i^0, v_i^0, p_i^0 and then, $v_{i+1/2}^0$ from Eqs. (2) to (17), and $p_{i+1/2}^0$ given by Eq. (26).

• Estimation step (first iteration: $k = n$)

Estimation of the density:

$$\varrho_i^\star = \varrho_i^n - \frac{\tau}{S_i}\left(\varrho_i^\star v_{i+1/2}^k S_{i+1/2} - \varrho_{i-1}^\star v_{i-1/2}^k S_{i-1/2}\right) \tag{34}$$

Estimation of the momentum: Eq. (28)

Estimated mass flux: Eq. (16)

Estimated interface velocity:

$$v_{i+1/2}^\star = \frac{(\varrho v)_{i+1/2}^\star}{\varrho_i^\star} \qquad \text{(upwinded value for the convective quantity } \varrho_{i+1/2}^\star) \tag{35}$$

Estimated total energy and total enthalpy:

$$(\varrho E)_i^\star = \frac{p_i^k}{\gamma - 1} + \frac{1}{2}(\varrho v)_i^\star \frac{(\varrho v)_i^\star}{\varrho_i^\star} \qquad \text{(case of a perfect gas)} \tag{36}$$

$$(\varrho H)_i^\star = (\varrho E)_i^\star + p_i^k \tag{37}$$

• Correction step

Solution of Eq. (27), rewritten as

$$A_{i-1}p'_{i-1} + A_i p'_i + A_{i+1}p'_{i+1} = \Sigma_i \tag{38}$$

where

$$A_{i-1} = -\frac{\tau}{S_i}[H_{i-1}^\star \frac{K_p}{f_c(M_{0,i-1/2}^\star)} \max\{1 - (\overline{M}_{i-1/2}^\star)^2\sigma, 0\} \frac{1}{c_{i-1/2}^\star} + \frac{\gamma}{\gamma - 1} c_{i-1/2}^\star M_{i-1/2}^\star \mathcal{P}^+(M_{i-1}^\star)] S_{i-1/2} \tag{39}$$

$$A_{i+1} = -\frac{\tau}{S_i}[H_i^\star \frac{K_p}{f_c(M_{0,i+1/2}^\star)} \max\{1 - (\overline{M}_{i+1/2}^\star)^2\sigma, 0\} \frac{1}{c_{i+1/2}^\star} - \frac{\gamma}{\gamma - 1} c_{i+1/2}^\star M_{i+1/2}^\star \mathcal{P}^-(M_{i+1}^\star)] S_{i+1/2} \tag{40}$$

$$A_i = \frac{1}{\gamma-1} + \frac{\tau}{S_i}\{[H_i^\star \frac{K_p}{f_c(M^\star_{0,i+1/2})} \max\{1-(\overline{M}^\star_{i+1/2})^2\sigma, 0\}\frac{1}{c^\star_{i+1/2}} + \frac{\gamma}{\gamma-1} c^\star_{i+1/2} M^\star_{i+1/2} \mathcal{P}^+(M_i^\star)]S_{i+1/2} + [H^\star_{i-1}\frac{K_p}{f_c(M^\star_{0,i-1/2})} \max\{1-(\overline{M}^\star_{i-1/2})^2\sigma, 0\}\frac{1}{c^\star_{i-1/2}} - \frac{\gamma}{\gamma-1} c^\star_{i-1/2} M^\star_{i-1/2} \mathcal{P}^-(M_i^\star)]S_{i-1/2}\} \quad (41)$$

and

$$\Sigma_i = -\{(\varrho E)_i^\star - (\varrho E)_i^n + \frac{\tau}{S_i}[(\varrho H)_i^\star c^\star_{i+1/2} M^\star_{i+1/2} S_{i+1/2} - (\varrho H)^\star_{i-1} c^\star_{i-1/2} M^\star_{i-1/2} S_{i-1/2}]\} \quad (42)$$

• Updates

$$p_i^{k+1} = p_i^k + p_i' \quad (43)$$

$$\varrho_i^{k+1} = \varrho_i^\star \quad (44)$$

$$(\varrho v)_i^{k+1} = (\varrho v)_i^\star + (\varrho v)_i' \quad (45)$$

where $(\varrho v)_i'$ is given by Eq. (33)

$$(\varrho E)_i^{k+1} = \frac{p_i^{k+1}}{\gamma-1} + \frac{1}{2}(\varrho v)_i^{k+1}\frac{(\varrho v)_i^{k+1}}{\varrho_i^{k+1}} \quad (46)$$

$p^{k+1}_{i+1/2}$ is evaluated by Eq. (26)
$c^{k+1}_{i+1/2}$ is evaluated using Eqs. (2)-(3)-(4)
$M^{k+1}_{i+1/2}$ is evaluated using Eqs. (15)-(19)

$$(\varrho v)^{k+1}_{i+1/2} = c^{k+1}_{i+1/2}\ M^{k+1}_{i+1/2}\ \varrho_i^{k+1} \quad (47)$$

$$v^{k+1}_{i+1/2} = \frac{(\varrho v)^{k+1}_{i+1/2}}{\varrho_i^{k+1}} \quad (48)$$

4 A LOW MACH STRATEGY FOR NONREFLECTING BOUNDARY CONDITIONS IN THE MODEL ALGORITHM

First, we recall a few elements of the characteristic analysis of the Euler equations. Then, the combination of the pressure correction method with the characteristic based nonreflecting treatment is described in detail.

4.1 Wave propagation: basic aspects

First, it is common to derive the following characteristic relations from the set (1) of equations (see Thompson[12]),

$$\mathrm{d}v - \frac{\mathrm{d}p}{\varrho c} = cv\ \mathrm{d}t\frac{\mathrm{d}_x S}{S} \qquad \text{on} \quad \Gamma_1 \ : \ \frac{\mathrm{d}x}{\mathrm{d}t} = v - c \tag{49a}$$

$$\mathrm{d}\varrho - \frac{1}{c^2}\mathrm{d}p = 0 \qquad \text{on} \quad \Gamma_2 \ : \ \frac{\mathrm{d}x}{\mathrm{d}t} = v \tag{49b}$$

$$\mathrm{d}v + \frac{\mathrm{d}p}{\varrho c} = -cv\ \mathrm{d}t\frac{\mathrm{d}_x S}{S} \qquad \text{on} \quad \Gamma_3 \ : \ \frac{\mathrm{d}x}{\mathrm{d}t} = v + c \tag{49c}$$

In the previous relations, the characteristic variables W_1, W_2 and W_3 appear such that

$$\mathrm{d}\begin{pmatrix} W_1 \\ W_2 \\ W_3 \end{pmatrix} = \begin{pmatrix} \mathrm{d}v - \frac{\mathrm{d}p}{\varrho c} \\ \mathrm{d}\varrho - \frac{\mathrm{d}p}{c^2} \\ \mathrm{d}v + \frac{\mathrm{d}p}{\varrho c} \end{pmatrix} = cv\ \mathrm{d}t\ \frac{\mathrm{d}_x S}{S}\begin{pmatrix} 1 \\ 0 \\ -1 \end{pmatrix} \tag{50}$$

Then, let us set

$$\mathcal{L}_1 = (v - c)(\partial_x v - \frac{1}{\varrho c}\partial_x p) \tag{51a}$$

$$\mathcal{L}_2 = v(\partial_x \varrho - \frac{1}{c^2}\partial_x p) \tag{51b}$$

$$\mathcal{L}_3 = (v + c)(\partial_x v + \frac{1}{\varrho c}\partial_x p) \tag{51c}$$

which verify the so-called LODI (for Laminar One Dimensional and Inviscid) equations,

$$\partial_t \varrho + \frac{\varrho}{2c}(\mathcal{L}_3 - \mathcal{L}_1) + \mathcal{L}_2 = -\varrho v\frac{\mathrm{d}_x S}{S} \tag{52a}$$

$$\partial_t v + \frac{1}{2}(\mathcal{L}_1 + \mathcal{L}_3) = 0 \tag{52b}$$

$$\partial_t p + \frac{\varrho c}{2}(\mathcal{L}_3 - \mathcal{L}_1) = -\varrho v c^2\frac{\mathrm{d}_x S}{S} \tag{52c}$$

It is worthwhile to note the following gradient expression,

$$\partial_x v = \frac{1}{2}\left(\frac{\mathcal{L}_1}{v - c} + \frac{\mathcal{L}_3}{v + c}\right) \tag{53}$$

4.2 Characteristic based boundary treatment

Now, let 0 and L be the inlet and outlet coordinates of the nozzle. When the outflow is subsonic, only the first characteristic variable can be subject to a nonreflecting boundary condition,

$$\partial_t W_1|_{x=L} = 0 \tag{54}$$

or equivalently, in spatial form,

$$\mathcal{L}_1|_{x=L} = \left(cv \frac{\mathrm{d}_x S}{S} \right)\Bigg|_{x=L} \tag{55}$$

For sake of simplicity, we consider a nozzle with a constant section at the inlet and at the outlet, so that the right hand side of Eq. (55) is zero. As usual, since the flow is supposed to be subsonic, values of the density and the velocity are imposed at the inlet, while a target value is given at the outlet for the pressure. Since

$$\mathrm{d}W_3 - \mathrm{d}W_1 = \frac{2}{\varrho c}\mathrm{d}p \tag{56}$$

the rate of change of the characteristic variable W_1 can not be set to zero at the outlet, because this could lead to an ill-posed problem when the pressure is imposed at this point. More precisely, for a fixed outlet pressure, the perfectly nonreflecting condition would require setting the outgoing acoustic wave to zero, where this wave should be estimated from the interior of the computational domain. Following Poinsot and Lele[9], a relaxation of the nonreflecting outlet condition can then be considered,

$$\mathcal{L}_1 = K\ (p^t - p) \tag{57}$$

where p^t and p are respectively the target and the current value of the pressure at the outlet. The relaxation coefficient K is related to a cut-off pressure frequency (see Selle *et al.*[11]). Since only high frequencies are concerned by the nonreflective treatment, reflection of acoustic fluctuations can be avoided while maintaining a given value for the mean pressure associated with low frequencies. Practically, following Ref. [11], where a frequency analysis in a duct is proposed, we take

$$K = \pi(1 - M_{\max}^2)/(\varrho L) \tag{58}$$

Here $M_{\max}$ is the maximum of the Mach number in the computational domain. For example, $M_{\max} = M_{\text{throat}}$ in the case of a subsonic nozzle with a variable section. With $\mathcal{L}_1$ given by Eq. (57) and with $\mathcal{L}_2$ and $\mathcal{L}_3$ estimated from the interior points of the computational domain, density, velocity and pressure are advanced in time on the boundary $x = L$, according to the set of equations (52).

4.3 Coupling of the LODI system and the model algorithm

We describe now the connection between the nonreflective treatment at the outlet and the pressure correction algorithm that we consider. Denoting by the superscript "nr" the nonreflecting values obtained by the procedure previously described, the following relations are used,

$$\varrho_N^\star = \varrho_N^{\rm nr} \tag{59}$$

$$(\varrho v)_N^\star = \varrho_N^{\rm nr} v_N^{\rm nr} \tag{60}$$

$$p'_N = p_N^{\rm nr} - p_N^n \tag{61}$$

For the momentum correction, we use Eq. (49a), or else, Eqs. (53) and (55),

$$\partial_x v = \frac{1}{\varrho c}\partial_x p \tag{62}$$

which lead to

$$(\varrho v)_N^{k+1} = \frac{(\varrho v)_{N-1}^{k+1}}{\varrho_{N-1}^{k+1}}\varrho_N^{k+1} + \frac{1}{\varrho_N^{k+1} c_N^{k+1}}(p_N^{\rm nr} - p_{N-1}^{k+1}) \tag{63}$$

where

$$c_N^{k+1} = \sqrt{\frac{\gamma p_N^{\rm nr}}{\varrho_N^{k+1}}} \tag{64}$$

Now considering the subsonic inflow, $\mathcal{L}_1$ can be estimated from the interior points. As $\partial_t v$ and $\partial_t \varrho$ are known, only the pressure has to be calculated at the next time step. This can easily be done from Eqs. (52b) and (52c). Because values of density and velocity at the inlet - denoted by $\varrho_{\rm in}$ and $v_{\rm in}$ - are prescribed, the inlet momentum is not corrected. Thus, the following relations are used,

$$\varrho_1^\star = \varrho_{\rm in} \tag{65}$$

$$(\varrho v)_1^\star = \varrho_{\rm in} v_{\rm in} \tag{66}$$

$$(\varrho v)'_1 = 0 \tag{67}$$

and for the pressure correction,

$$p'_1 = p_1^{\rm nr} - p_1^n \tag{68}$$

5 NUMERICAL EXPERIMENTS

Two cases are considered in this section. The first one, concerning a wave packet propagation, allows to check the nonreflecting property that we claimed. The second one, by considering a steady flow in a nozzle with a variable section, was chosen to compare the convergence rates and the time step limitations for the nonreflecting treatment and a classical set of absorbing boundary conditions. Practically, we take

$$\tau = \frac{\mathrm{CFL}_v}{v_{\max}}$$

where CFL_v is chosen and $v_{\max}$ is the maximal velocity in the computational domain.

5.1 Acoustic wave packet propagation

An acoustic wave packet is generated through an initial acoustic gaussian perturbation superimposed onto a mean flow, with a constant density ϱ_0, velocity v_0 and pressure p_0, in a one meter long nozzle with a constant section. Thus, $p = p_0 + \delta p$, where at $t = 0$,

$$\delta p = A \exp(-\frac{(x-m)^2}{2s^2})$$

By taking

$$\delta v = \frac{\delta p}{\varrho_0 c_0} \quad , \quad \delta \varrho = \frac{\delta p}{c_0^2}$$

we obtain a wave packet that travels towards the outlet of the nozzle. The dimensional numerical settings for the wave generation are given in Table 1. The other parameters for the computation are given in Table 2.

A (Pa)	s (m)	m (m)	p_0 (Pa)	v_0 (m/s)	ϱ_0 (kg / m^3)	N
1 000	2	50	101 300	0.3089	1.2046	100

Table 1: Settings for the acoustic wave packet generation

First, one observes in Figs. 1 to 3 the amplitude decrease and the phase distorsion of the wave. These reveal the dissipative and dispersive features of the scheme described in Sec. 3.

CFL$_v$	M$_{\text{in}}$	K_p	K_v	σ
3×10^{-7}	9×10^{-4}	10^{-3}	10^{-4}	1

Table 2: Settings for the acoustic wave packet propagation

Focusing on the outlet nonreflecting treatment, we verify that the wave packet leaves the computational domain. However, the evacuation of the wave is not complete. From the numerous computations that we done, not shown here, it appears that the residual highly depends on the calibration of the relaxation coefficient K (see Eq. (58)). Let us recall that in the present paper, the calibration adopted is the one suggested in the Ref. [11].

5.2 Low Mach number steady flow

Here, our purpose is to examine, *(1)* to what extent the nonreflecting boundary treatment does affect the time step limitation, which is an important argument for using the semi-implicit algorithms; *(2)* the comparison between nonreflecting and absorbing boundary conditions with regard to the numerical precision. A steady flow in a nozzle with a

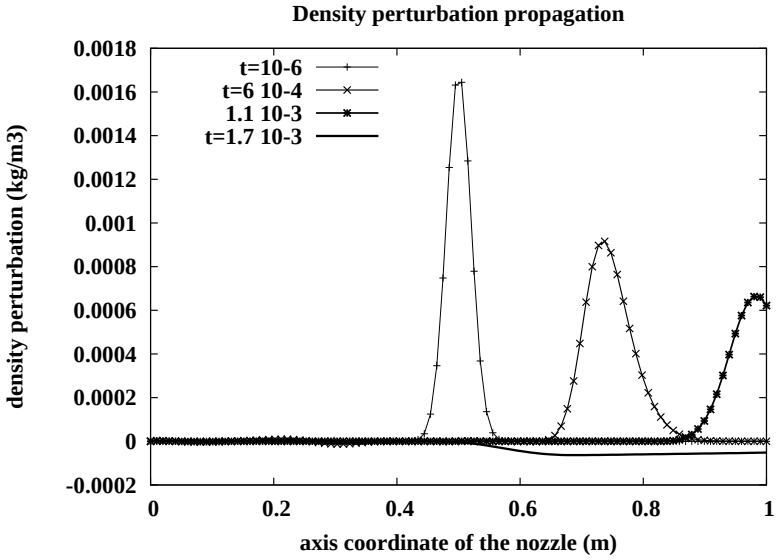

Figure 1: Density perturbation distribution along the nozzle - $t = 10^{-6}, 6\times10^{-4}, 1.1\times10^{-3}$ and 1.7×10^{-3}

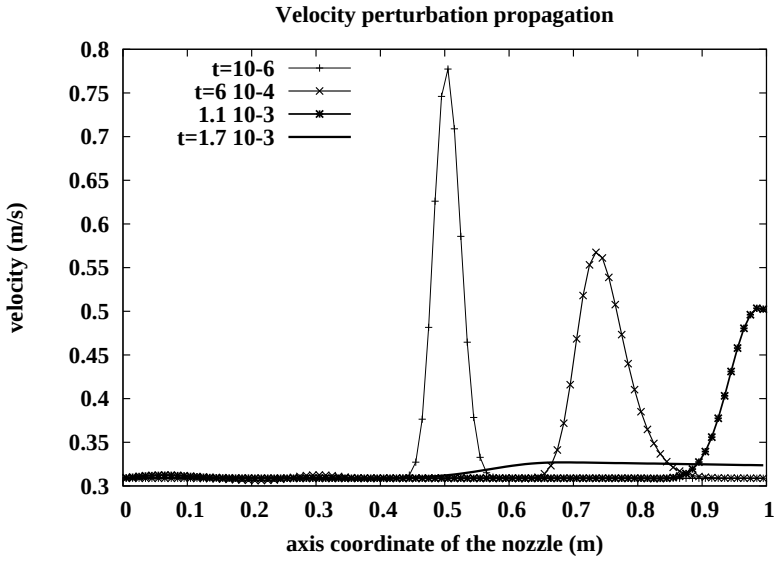

Figure 2: Velocity perturbation distribution along the nozzle - $t = 10^{-6}, 6\times10^{-4}, 1.1\times10^{-3}$ and 1.7×10^{-3}

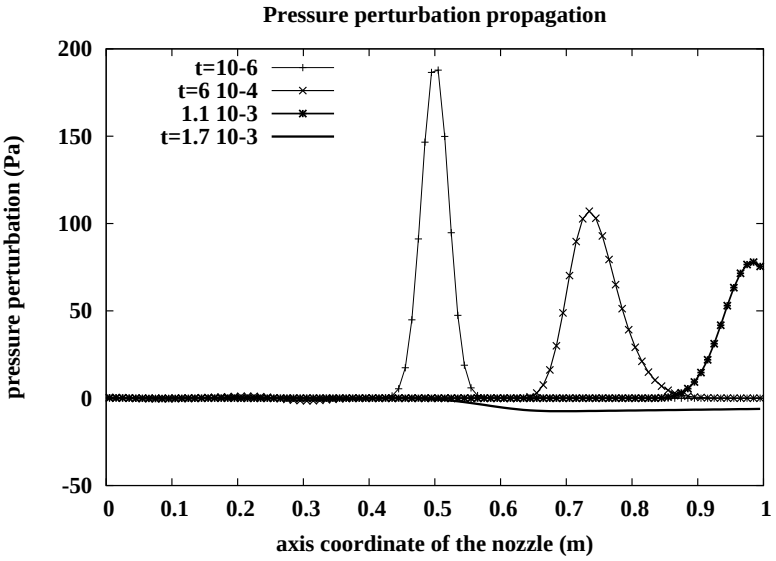

Figure 3: Pressure perturbation distribution along the nozzle - $t = 10^{-6}, 6\times10^{-4}, 1.1\times10^{-3}$ and 1.7×10^{-3}

variable section, given by

$$S(x) = \begin{cases} 0.1, & 0 \leq x \leq 2/28 \\ 0.1\left\{0.9 + 0.1\left[2\left(\frac{x-\frac{11}{28}}{\frac{9}{28}}\right)^2 - \left(\frac{x-\frac{11}{28}}{\frac{9}{28}}\right)^4\right]\right\}, & 2/28 \leq x \leq 20/28 \\ 0.1, & 20/28 \leq x \leq 1 \end{cases}$$

is considered. The other settings are given in Table 3. The maximum allowable acoustic CFL number is determined numerically as $\mathrm{CFL}_{v+c} \simeq 2$. The numerical results, when we use the pressure correction method in combination with the characteristic based nonreflecting boundary conditions (refered as 'PC & CBNR' in the labels of the figures), are very close to the analytical ones (see Figs. 4 and 5).

$\mathrm{M}_{\mathrm{throat}}$	K_p	K_v	σ	N
0.04	4.5×10^{-2}	10^{-4}	1	100

Table 3: Settings for the low Mach number steady flow with nonreflecting boundary treatment

Incidentally, the capability of the algorithm described in Sec. 3 to overcome the checkerboard decoupling that can arise in low Mach number computations is checked.

A comparison between the nonreflecting treatment and absorbing boundary conditions, such that

$$\partial_x p|_{x=0} = 0 \quad , \quad \partial_x v|_{x=L} = 0 \tag{69}$$

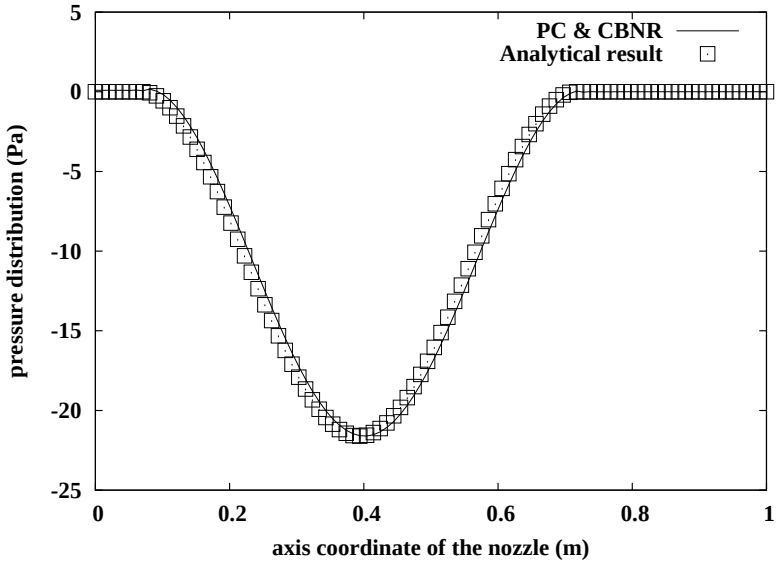

Figure 4: Pressure distribution along the nozzle - $\mathrm{CFL}_{v+c} \simeq 2$

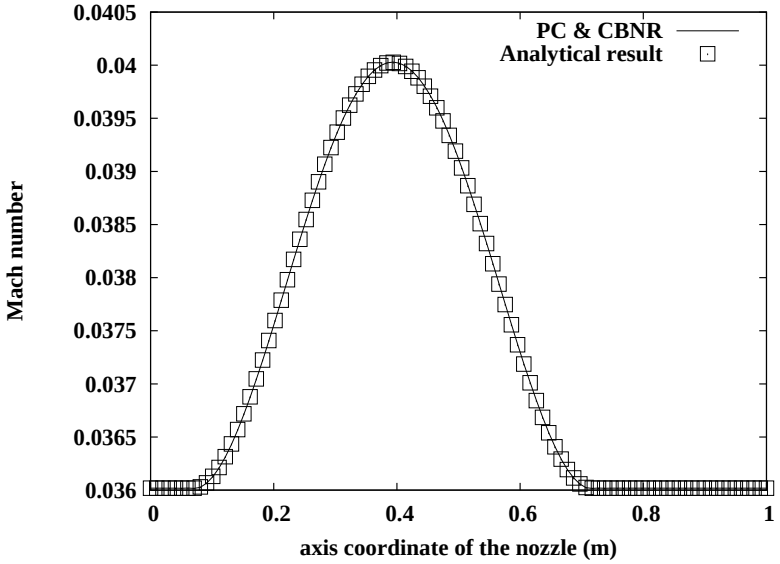

Figure 5: Mach number along the nozzle - $\mathrm{CFL}_{v+c} \simeq 2$

is given in Figs. 6 to 8. Note that the dissipation coefficient K_p had to be increased to 1.5 for the computation with the absorbing boundary conditions (69). When comparing the residuals of the mass, momentum and energy equations, one observes that the residuals are smaller at every time step when using the nonreflecting treatment. This is also true for the other computations we made, not shown in the present paper.

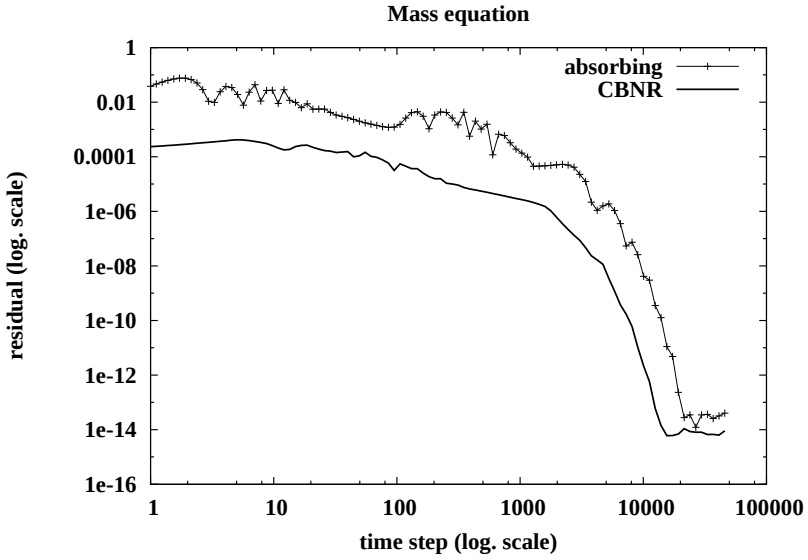

Figure 6: Residuals of the mass equation with absorbing and nonreflecting boundary conditions - $\mathrm{CFL}_{v+c} \simeq 2$

From numerous computations not shown in this paper, it appears that the choice of the boundary treatment does affect the time step limitation, which is stronger when using the absorbing boundary conditions (69) than for the nonreflecting approach described in the previous section. However, since this later approach allows an acoustic CFL larger than unity, its combination with semi-implicit algorithms is of interest. Moreover, in this case the residuals are smaller than the ones obtained with the absorbing boundary conditions at almost every time step. Thus, we can consider that the numerical precision is better with the nonreflecting treatment. Note however that the first and last nodes of the mesh were excluded in the residuals computations presented in Figs. 6 to 8, since they coincide with the boundary of the computational domain according to our discretization (see Sec. 2). Therefore, no flux is defined at one side of the first and last cells.

The nonreflecting values p_1^{nr}, ϱ_N^{nr}, v_N^{nr} and p_N^{nr} (see paragraph 4.3) are calculated at the beginning of each time step. Focusing on the first one, one observes in Figs. 6 to 8 that their integration into the pressure correction algorithm allows to improve the precision from the very first time loop.

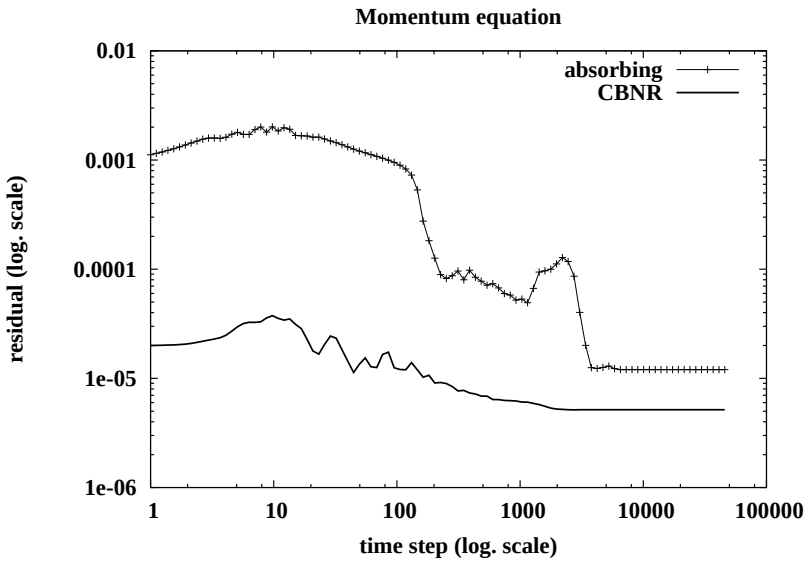

Figure 7: Residuals of the momentum equation with absorbing and nonreflecting boundary conditions - $\mathrm{CFL}_{v+c} \simeq 2$

Finally returning to the discussion on the time step limitation, one observes that the maximal allowable acoustic CFL that we obtained ($\mathrm{CFL}_{v+c} \simeq 2$) is lower than the one of Wall *et al.*[14] ($\mathrm{CFL}_{v+c} = 40$). Let us note however that these authors used low dissipative interpolation schemes, for which numerical difficulties such as the checkerboard decoupling could occur for Mach number lower than 0.04.

6 CONCLUSION

A characteristic based nonreflecting treatment is found to be not straightforward for SIMPLE-type algorithms employed for the governing equations of compressible flows. This is due to the time staggered updating of the physical variables. Accordingly, the nonreflecting values, which are calculated at the beginning of each time loop from the LODI equations, are applied in the pressure correction scheme in a carefully chosen sequential order.

The capability of the suggested methodology for coupling the LODI system and a SIMPLE-type model algorithm was illustrated for two generic test cases. The results proved to be quite encouraging and it seems possible to apply this technique to complex boundary conditions while preserving some advantages of the classical absorbing treatment.

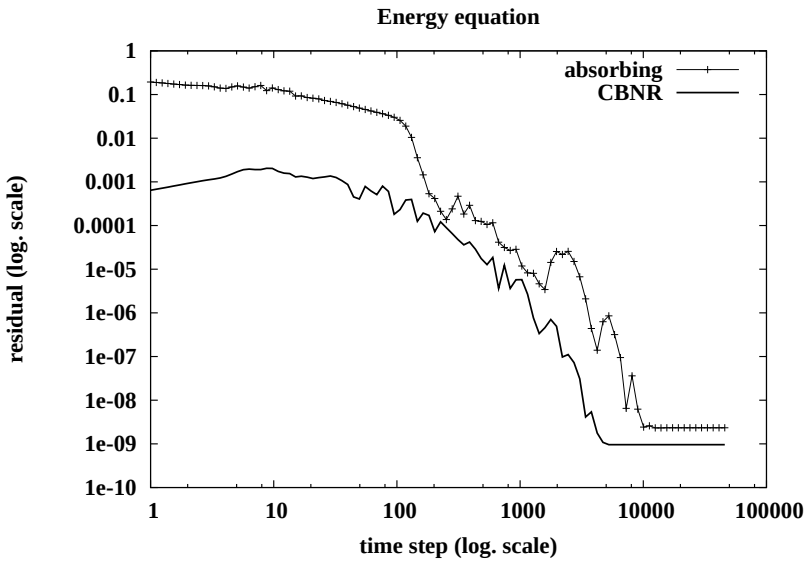

Figure 8: Residuals of the energy equation with absorbing and nonreflecting boundary conditions - $\mathrm{CFL}_{v+c} \simeq 2$

REFERENCES

[1] M. Baum, T. Poinsot and D. Thévenin, Accurate Boundary Conditions for Multicomponent Reactive Flows, *J. Comp. Phys.*, **116**, 247–261 (1994).

[2] J. R. Edwards and M.-S. Liou, Low-Diffusion Flux-Splitting Methods for Flows at All Speeds, *AIAA J.*, **36**(9), 1610–1617 (1998).

[3] Y. Hou and K. Mahesh, A robust colocated, implicit algorithm for direct numerical simulation of compressible, turbulent flows, *J. Comp. Phys.*, **205**, 205–221 (2005).

[4] M.-S. Liou, A Sequel to AUSM, part II: AUSM$^+$-up for all speeds, *J. Comp. Phys.*, **214**, 137–170 (2006).

[5] Y. Moguen, T. Kousksou, E. Dick and P. Bruel, On the role of the numerical dissipation in unsteady low Mach number flows computations, *submitted to ICCFD St-Petersburg 2010*

[6] B. Müller, Low Mach number asymptotics of the Navier-Stokes equations and numerical implications, *von Karman Institute for Fluid Dynamics*, 30$^{\text{th}}$ Computational Fluid Dynamics, Lecture Series 1999-03 (1999).

[7] K. Nerinckx, J. Vierendeels and E. Dick, A pressure-correction algorithm with Mach-uniform efficiency and accuracy, *Int. J. Numer. Meth. Fluids*, **47**, 1205–1211 (2004).

[8] K. Nerinckx, J. Vierendeels and E. Dick, Mach-uniformity through the coupled pressure and temperature correction algorithm, *J. Comp. Phys.*, **206**, 597–623 (2005).

[9] T. J. Poinsot and S. K. Lele, Boundary Conditions for Direct Simulations of Compressible Viscous Flow, *J. Comp. Phys.*, **101**, 104–129 (1992).

[10] D. H. Rudy and J.C. Strikwerda, A Nonreflecting Outflow Boundary Condition for Subsonic Navier-Stokes Calculations, *J. Comp. Phys.*, **36**, 55–70 (1980).

[11] L. Selle, F. Nicoud and T. Poinsot, Actual Impedance of Nonreflecting Boundary Conditions: Implications for Computation of Resonators, *AIAA J.*, **42**(5), 958–964 (2004).

[12] K. W. Thompson, Time Dependent Boundary Conditions for Hyperbolic Systems, *J. Comp. Phys.*, **68**, 1–24 (1987).

[13] D. R. van der Heul, C. Vuik and P. Wesseling, A conservative pressure-correction method for flow at all speeds, *Comput. Fluids*, **32**, 1113–1132 (2003).

[14] C. Wall, C. D. Pierce and P. Moin, A Semi-implicit Method for Resolution of Acoustic Waves, *J. Comp. Phys.*, **181**, 545–563 (2002).